Green Chemistry

PAPER

View Article Online
View Journal | View Issue

Cite this: *Green Chem.*, 2025, **27**, 3706

Electrolyte pH modulation for efficient and durable electrochemical cement clinker precursor production†

Lei Xu,[a,b] Lei Liu,[*b,c,d,e] Zheng Fang,[b,f] Min Chen,[a] Guangfeng Ou,[b,g] Michio Suzuki[h] and Yuya Sakai[b]

Cement production is carbon intensive and accounts for 7–8% of global CO_2 emissions. Deep cement decarbonization can be achieved if limestone calcination is replaced with an ambient-temperature electrochemical process. A big challenge of this process is the significant deposition of the $Ca(OH)_2$ product on the membrane, causing unacceptable operational durability and energy efficiency. To address this issue, we designed a two-chamber membrane-based cement clinker precursor electrolyzer. The electrolyte pH modulation and its effect on decarbonization, precipitation, and cell voltage are investigated. We reveal a thin $Ca(OH)_2$ layer on the anode side of the membrane under fast decarbonization kinetics (99% current efficiency) at a pH of 5.1, increasing the cell voltage by 50%. A periodic pH change using intermittent stirring ensures a relatively constant voltage level with a sacrifice of ~3% decarbonization efficiency. Membrane clogging is extremely significant in the cathode chamber due to the extreme pH environment (12.4), causing an inferior production rate of $Ca(OH)_2$ (59% of the theoretical limit). Introducing Ca^{2+} into the catholyte leads to a much lower pH (11.8) and a clean membrane throughout the electrolysis, increasing the current efficiency for $Ca(OH)_2$ production to 84%. Our work demonstrates a viable approach for efficient and durable production of electrochemical cement clinker precursors.

Received 13th December 2024,
Accepted 27th February 2025

DOI: 10.1039/d4gc06322h

rsc.li/greenchem

Green foundation

1. This work introduces an electrochemical process to produce a low-carbon cement clinker precursor [$Ca(OH)_2$] from limestone for deep cement decarbonization.
2. We achieved a lower catholyte pH and a clean membrane throughout the electrolysis by tailoring the electrolyte composition, solving the membrane clogging problem at an extreme pH and leading to the highest production rate of $Ca(OH)_2$ ever reported in the literature.
3. Future research will be dedicated to optimizing the Ca^{2+} transference number, cathode current efficiency, and cell voltage, especially in large-scale operations.

1. Introduction

Cement is the most consumed manufactured material worldwide.[1] We produced around 4 billion tonnes of cement every year in the past ten years. This number is expected to increase up to 4.7 billion tonnes by 2050.[1–3] Such huge production leads to a high carbon intensity, which accounts for 7–8% of global CO_2 emissions, primarily from cement clinker production.[4–6] Modern cement clinker manufacturing mainly consists of two steps:[3] first, the chemical decomposition of limestone ($CaCO_3$) into lime (CaO) in a "precalciner" at temperatures over 800 °C; second, the manufacture of cement clinker in a rotary kiln heated up to ~1450 °C, producing a mixture of alite ($3CaO{\cdot}SiO_2$), belite ($2CaO{\cdot}SiO_2$) and other minerals from the pre-calcined feedstock. The calcination of limestone contributes 60%–70% of the total carbon emissions for

[a]*Key Laboratory for Ecological Metallurgy of Multimetallic Mineral (Ministry of Education), Northeastern University, Shenyang 110819, China*
[b]*Institute of Industrial Science, The University of Tokyo, 4-6-1 Komaba, Meguro, Tokyo 153-8505, Japan*
[c]*Engineering Research Center of Nano-Geomaterials of Ministry of Education, China University of Geosciences, Wuhan 430074, China. E-mail: liu-lei@cug.edu.cn*
[d]*Faculty of Materials Science and Chemistry, China University of Geosciences, Wuhan 430074, China*
[e]*Laboratory of Advanced Mineral Materials, China University of Geosciences, Wuhan 430074, China*
[f]*College of Materials Science and Engineering, Chongqing University, Chongqing 400045, China*
[g]*Department of Research and Development, Foshan Huijiang Concrete Corporation, China*
[h]*Department of Applied Biological Chemistry, Graduate School of Agricultural and Life Sciences, The University of Tokyo, 1-1-1 Yayoi, Bunkyo, Tokyo 113-8657, Japan*
†Electronic supplementary information (ESI) available. See DOI: https://doi.org/10.1039/d4gc06322h

clinker production, while the remaining 30%–40% mainly comes from fossil fuel combustion and electricity consumption.[3,5,7] The latter emission can be easily reduced using renewable and clean energy. However, the elimination of CO_2 generated during limestone decomposition seems very difficult. Several strategies are proposed to reduce the carbon footprint of cement production.[3–11] The replacement of limestone or cement clinker with low-carbon raw materials, such as natural pozzolans and calcium-rich industrial by-products (calcium carbide slag, blast furnace slag, coal fly ash, *etc.*), is the most direct and effective way for carbon emission reduction.[9] However, the substitution ratio for cement clinker is limited, and the quantity of high-quality alternatives is far from enough to meet the demands of cement production.[3,7,10] Carbon capture and sequestration (CCS) technology provides another viable approach, which includes CO_2 separation from the flue gas mainly using amine-based solvents and the subsequent storage of CO_2 through geological and oceanic sequestration or mineral carbonation methods.[3,5,8,10] However, the flue gas generated from the cement process is rather impure and its CO_2 concentration is usually below 25%, leading to low capture efficiency or a very high cost.[2,3,8,11] Besides, the scalability and stability of this process still face big challenges.

With continuous improvement in the cost-effectiveness and reliability of renewable electricity, the electrochemical-based method appears to be an emerging technology for green cement production. Ellis and coworkers first reported this approach in an H-cell using platinum electrodes and aqueous electrolytes.[2] In this reactor, neutral water electrolysis produces a steep pH gradient where limestone is dissolved in the acidic anolyte and $Ca(OH)_2$ is precipitated in the alkaline solution at the cathode.[2,12] They also confirmed the viability of manufacturing cement clinker using the produced $Ca(OH)_2$ as a precursor. The by-product H_2 gas is an excellent low-carbon fuel for cement clinker sintering, therefore eliminating the use of fossil fuels during the whole manufacturing process. Besides, the CO_2 produced during electrochemical decarbonization can be readily separated due to the inherently concentrated gas streams (~67% concentration). These distinguishing features would reduce the carbon emissions of cement production by over 90% if using renewable electricity.[2,13] A scheme of the electrochemical-based, low-carbon emission cement production process is presented in Fig. 1. Inspired by this work, Xie *et al.* proposed an integrated process using an electrochemical pulsed method to transform $CaCO_3$ into $Ca(OH)_2$ while *in situ* converting the generated CO_2 into valuable carbonaceous products (such as CO, formate, methane, *etc.*).[14] To improve the capture of the produced CO_2, Zhang along with others built a three-compartment electrochemical reactor with flowing electrolytes, by which ~100% current efficiency and a pure CO_2 stream were obtained at a cell voltage of 2.9 V and a current density of over 100 mA cm^{-2}.[15] They further achieved a much lower cell voltage (1.8 V at 100 mA cm^{-2}) by transforming the by-product H_2 into H^+ for $CaCO_3$ decomposition, significantly reducing the production cost.[16]

Although an ideal operating voltage and ~100% current efficiency for $CaCO_3$ decomposition proved to be possible in the electrochemical decarbonization reactor, the previous studies failed to quantify the output of the product $Ca(OH)_2$ owing to its significant adhesion on the membrane.[2,13,15–17] Instead, they used some indirect indexes (such as the generation rate of CO_2 at the electrode) to evaluate the production rate. Ramirez-Amaya *et al.* first measured the mass of the electrochemically produced $Ca(OH)_2$ and found that the conver-

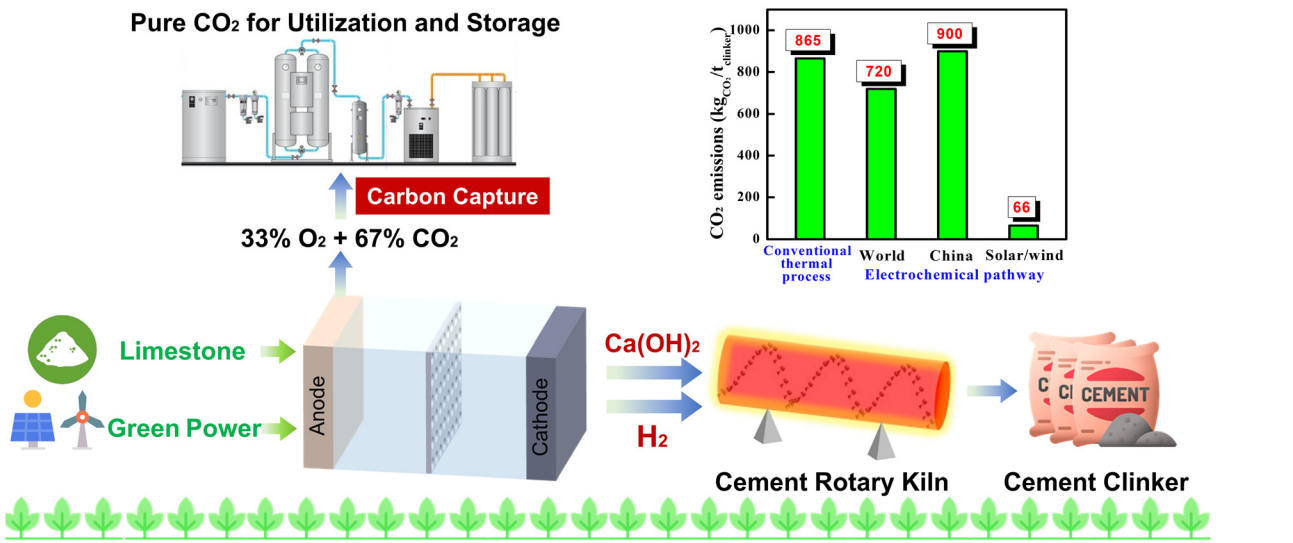

Fig. 1 A scheme of the electrochemical-based, low-carbon emission cement clinker production process. The carbon emissions during this process only come from electricity consumption, which can be reduced by over 90% at a cell voltage of 2.5 V and a current efficiency of 90% if using green electricity. Grid emission factors: world = 0.43 kg CO_2 per kW per h, China = 0.54 kg CO_2 per kW per h, solar or wind energy = 0.04 kg CO_2 per kW per h.[2,13,15–17]

sion rate of $CaCO_3$ to $Ca(OH)_2$ was below 30%.[18] Although periodic cleaning using mechanical or chemical methods provides a means for removing the accumulated deposits, it will degrade the process efficiency as well as the membrane performance and lifetime. Here, we design a new but simple membrane-based cement clinker precursor electrolyzer that operates at variable pH values to understand what role the electrolyte pH plays in the electrochemical process and how to control it. The most distinguishing feature of this approach is the absence of deposits on the membrane during electrolysis, by which we achieve a $Ca(OH)_2$ production rate of 1150 mg h^{-1} at 180 mA cm^{-2} with a current efficiency up to 84%. This efficiency is the highest ever reported in the literature. The self-cleaning of the membrane and the significant promotion of production rate under controlled electrolyte pH are significant advances over the previous studies.

2. Materials and methods

2.1 Chemicals, materials and electrolyzer design

The electrolysis process in this work was performed in a self-designed H-type cement clinker precursor production electrolyzer with an inner size of 14 cm × 14 cm × 4 cm, as shown in Fig. S1.† A porous plate coated with a cation exchange membrane (CEM) was used to separate the anode and cathode chambers and avoid solution and product contamination. Two platinum plates (5 cm × 2.5 cm × 0.01 cm) were used as the electrodes because of their high catalytic activity for water splitting, and they were connected to a direct-current voltage to supply power. The anode and cathode chambers were fed with 200 mL of 0.5 M $Ca(NO_3)_2$ solution and 300 ml of 1.0 M $NaNO_3$ solution with various Ca^{2+} concentrations, respectively. It is well known that H_2O (H^+) has a greater tendency to gain electrons than NO_3^-, Na^+, and Ca^{2+} at the cathode. Therefore, the added ions in the electrolytes will not participate in the electrode reactions and only water electrolysis occurs even at high voltages.[2] Na^+ and K^+ will participate in the electromigration process if a Na- or K-salt is used in the anolyte, affecting the transference number of Ca^{2+}. To avoid this issue and ensure a high Ca^{2+} transference number, we used Ca^{2+} as the sole cation in the anolyte. At the cathode, the initial Ca^{2+} concentration in the electrolyte regulates the pH and the product precipitation behavior. 5.60 g of commercial $CaCO_3$ powder (purity > 99.5%) was added to the anode chamber before electrolysis.

2.2 Production and characterization of electrochemical $Ca(OH)_2$

We conducted electrolysis experiments at a constant current (1 A with a current density of ~180 mA cm^{-2} to ensure a high enough yield of the electrochemical product). During electrolysis, the system voltage and electrolyte pH were recorded every 10 min to determine their correlation (the interval is 5 min in the first 30 min). Magnetic stirring (500 rpm) was applied in the anode chamber during electrolysis to accelerate the reaction between $CaCO_3$ and the generated acid. The cathode produces hydroxide ions and gaseous H_2 during electrolysis, and the former will combine with the Ca^{2+} delivered from the anode to form $Ca(OH)_2$ precipitates. All the tests were conducted at ambient temperature and pressure. After several hours of electrolysis, the slurry in each chamber was collected and transferred into a beaker using a 20 ml dropper, and then the $Ca(OH)_2$ products were weighed and characterized by XRD, SEM and TG-DTA after washing, filtration and drying. The metal ion concentrations in the electrolytes before and after electrolysis were measured by inductively coupled plasma mass spectroscopy (ICP-MS). eqn (S1)–(S3)† show the calculation methods of the decarbonization efficiency of $CaCO_3$, the current efficiency for $Ca(OH)_2$ production and the Ca^{2+} transference number, respectively.

3. Results and discussion

3.1 Influence of anolyte pH on the decarbonization efficiency and cell voltage

We controlled the pH in the anolyte [0.5 M $Ca(NO_3)_2$] by adjusting the stirring frequency. The current efficiency of the decarbonization reactor and cathode chamber was calculated by comparing $CaCO_3$ mass loss and $Ca(OH)_2$ output, respectively, with the theoretical moles of H_2 produced at the cathode.[2] Fig. 2a shows the pH evolution of the anolyte with time at various stirring frequencies. The pH reaches its constant level quickly and remains at around 5.1 when stirring is continuous during electrolysis. The slightly acidic environment suggests that the decarbonization of $CaCO_3$ is very fast when using an electrochemical process under favorable kinetics. This feature leads to an extremely high current efficiency (~99%) for the electrochemical decomposition of $CaCO_3$ (Fig. 2b), with the complete consumption of the added $CaCO_3$ powder which is in equivalent moles to the H_2 produced during electrolysis (Fig. S2†). Zhang, along with others,[13,15,16] confirmed a similar finding that almost all of the protons produced by the oxygen evolution reaction during water electrolysis can participate in the decarbonization reaction.

When stirring is stopped, the anolyte pH declines rapidly first until it reaches around 1 and then shows a slight but continuous decrease (Fig. 2a). The accumulated H^+ can be consumed in seconds when stirring starts at the end of electrolysis, increasing the pH to around 5.0. Even so, the current efficiency for decarbonization is only 84.7% in this case (Fig. 2b). This demonstrates that some of the H^+ ions generated at the anode were transported across the CEM to the cathode chamber driven by electric potential, where they would recombine with OH^- to form water.[2] This reaction also leads to a significantly lower Ca^{2+} transference number and current efficiency for $Ca(OH)_2$ production (Fig. 2b). The pH shows a periodic variation with electrolysis time (from 5–1) using an intermittent stirring method. Fortunately, this operation only causes a slight reduction in the decarbonization efficiency and production rate, suggesting that the electromi-

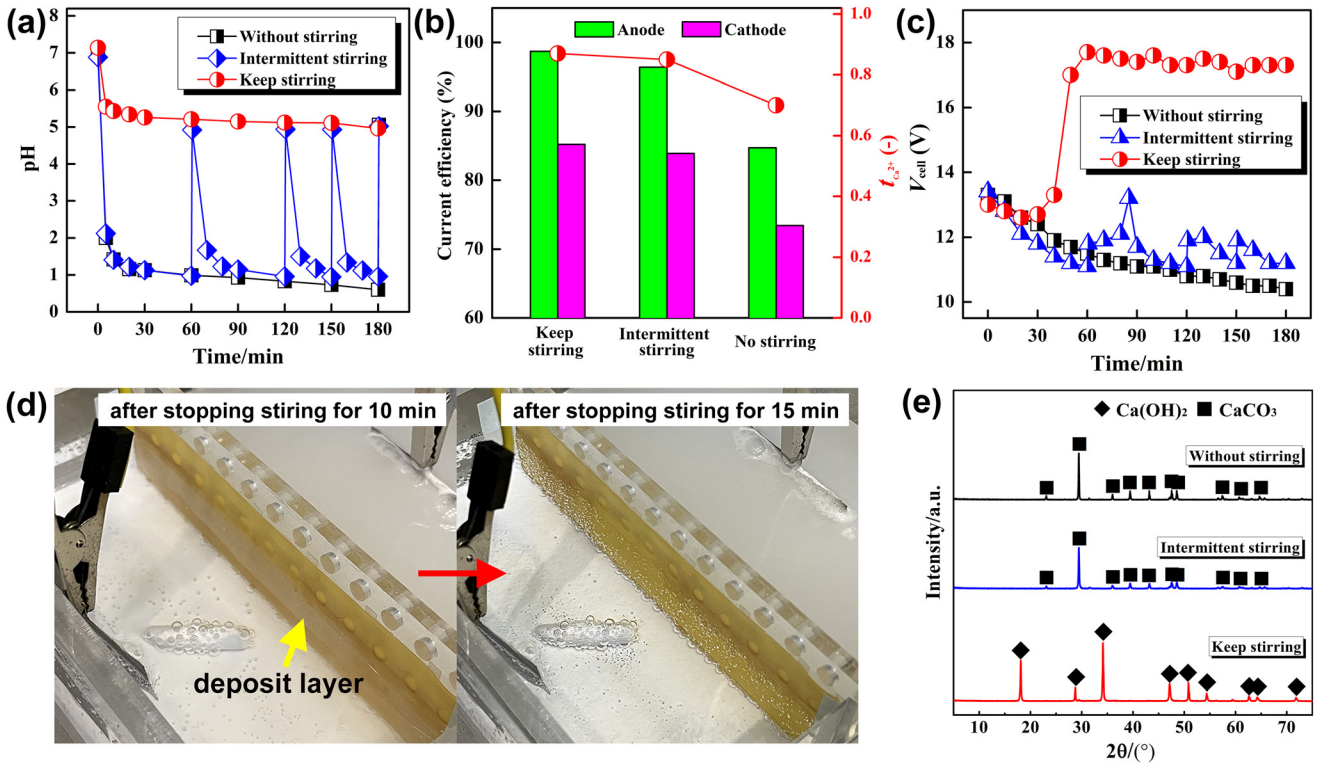

Fig. 2 Operating characteristics of the electrochemical decomposition process of $CaCO_3$ at various anolyte pH values with 0.5 M $Ca(NO_3)_2$ solution as the anolyte and 1.0 M $NaNO_3$ + 0.2 M $Ca(NO_3)_2$ solution as the catholyte. (a) Evolution of the anolyte pH with time at various stirring frequencies. (b) Measured anode and cathode current efficiency based on $CaCO_3$ consumption and $Ca(OH)_2$ output, respectively. (c) Voltage–time curves for the cement clinker precursor electrolyzer with various stirring frequencies. (d) Formation and disappearance of the deposit layer at the anode side of the membrane when using intermittent stirring. (e) XRD patterns of the residues collected from the anode chamber and membrane after electrolysis for 3 h.

gration of H^+ under significantly acidic solutions can be mitigated as long as its accumulation can be periodically eliminated by stirring.

Although the weak acidic environment in the anode chamber caused by full-time stirring ensures a high current efficiency, it gives rise to a sudden and dramatic increase of cell voltage after electrolysis for 30 min, as shown in Fig. 2c. However, the cell voltage notably decreases with time without any stirring. This trend is mainly associated with the corresponding change in anolyte pH (Fig. 2a) since the increased concentration of H^+ contributes to a high conductivity because it is regarded as an ideal charge carrier owing to its excellent ion mobility.[19,20] The generally high voltage is caused by the large current density and the unoptimized electrolyzer. Similar to the pH variation, a periodic change in the voltage is detected when intermittent stirring is performed. Although a sudden increase in voltage is also observed after short-term stirring, the voltage level is significantly lower than that under constant stirring. After stopping stirring, we found a white thin deposit layer at the anode side of the membrane, as shown in Fig. 2d. This layer obstructs the metal ion transport through the CEM and is responsible for the voltage fluctuation. Fortunately, this precipitate layer disappeared after standing for several minutes, leading to a sharp drop in the cell voltage.

The above results and observations suggest that pH variation at the anode is critical to the current efficiency and cell voltage. We collected the white deposits from the membrane directly after electrolysis under continuous stirring. Upon washing, filtration, and drying, we verified this product to be $Ca(OH)_2$ by X-ray diffraction (XRD) (Fig. 2e). As mentioned before,[2] a large pH gradient is produced between the two chambers during electrolysis. Although the CEM prevents the transport of anions under an electric field, several OH^- ions will migrate toward the anode chamber due to their high mobility and high concentration.[21] They will block the membrane by reacting with the Ca^{2+} nearby to form precipitates. The dissolution of $Ca(OH)_2$ requires a low pH (~1.6) because its saturated solution is highly alkaline (pH = 12.4).[22] Therefore, the weak acidic environment under fast decarbonization kinetics could not dissolve the deposits, causing their stable existence on the membrane and increasing the cell voltage even though it is very thin. Fortunately, the rapid accumulation of H^+ after stopping stirring achieves the self-cleaning of the membrane since the pH reaches below 1.6 quickly, leading to a relatively flat voltage profile (Fig. 2a and c). The results indicate that the anolyte pH during electrochemical cement clinker production should be kept at an appropriate level. Otherwise, the decarbonization reaction or cell voltage will be significantly affected. In other words, it is

necessary to sacrifice some of the anode current efficiency for better energy efficiency. Besides, a lower liquid-to-solid ratio helps to slow down the declining trend of anolyte pH, by which the voltage level can be further reduced with the current efficiency being maintained above 93% (Fig. S3†). Therefore, adequate limestone supply to the electrolyzer is necessary to create a better balance between current efficiency and cell voltage.

3.2 Influence of catholyte pH on the production rate and process stability

Having demonstrated the role of anolyte pH in current efficiency and cell voltage, we also attempted to understand what role the catholyte pH plays in the electrochemical process and how to control it. We measured the pH in the cathode chamber with 1.0 M $NaNO_3$ solution as the electrolyte during electrolysis and found that it increased rapidly in the first 5 min (≥11.5, Fig. 3a). The growth rate of pH slows down with time, and it remains at a constant value of 12.4 beyond 60 min of electrolysis. The high pH enables the Ca^{2+} transported from the anode chamber to separate as $Ca(OH)_2$ by reacting with OH^-, completing the cement clinker precursor production.[2] It can be seen that the precipitation behavior is evident across the whole area of the cathode chamber (Fig. 4a and Movie S1†). Meanwhile, the product also significantly precipitates on the membrane of this chamber, leading to significant blockage of the transport channels and a rapid increase in voltage after electrolysis for several hours (Fig. 3b and 4a).

The membrane clogging is common for the electrochemical decarbonization reactor if a Na- or K-salt is used as the cathode electrolyte. Many researchers regard it as a significant challenge to operational durability.[2,13,15,17] To address this issue, periodic cleaning of the precipitation product on the membrane was performed using a wiper insert, mechanical stirring, or acid treatment,[13,17,23] by which the cell voltage can be maintained at a constantly low level. By far, however, no study in the literature has tried to mitigate or even completely prevent the precipitate accumulation on the membrane. It seems like this phenomenon is inevitable because of the extreme pH environment in the cathode chamber.[24] To avoid this phenomenon, Zhang *et al.* transferred the electrochemically produced Ca^{2+} and OH^- into a distinct chemical reactor to form $Ca(OH)_2$ instead of precipitating within the electrolyzer.[25] This is a possible solution, but it makes the process more complicated.

To understand the nature of the adhesion mechanism of the product on the membrane, we made the following calculations. During direct-current electrolysis using a CEM as the separator, one mole of Ca^{2+} will migrate into the cathode chamber for every two moles of OH^- produced at the cathode.

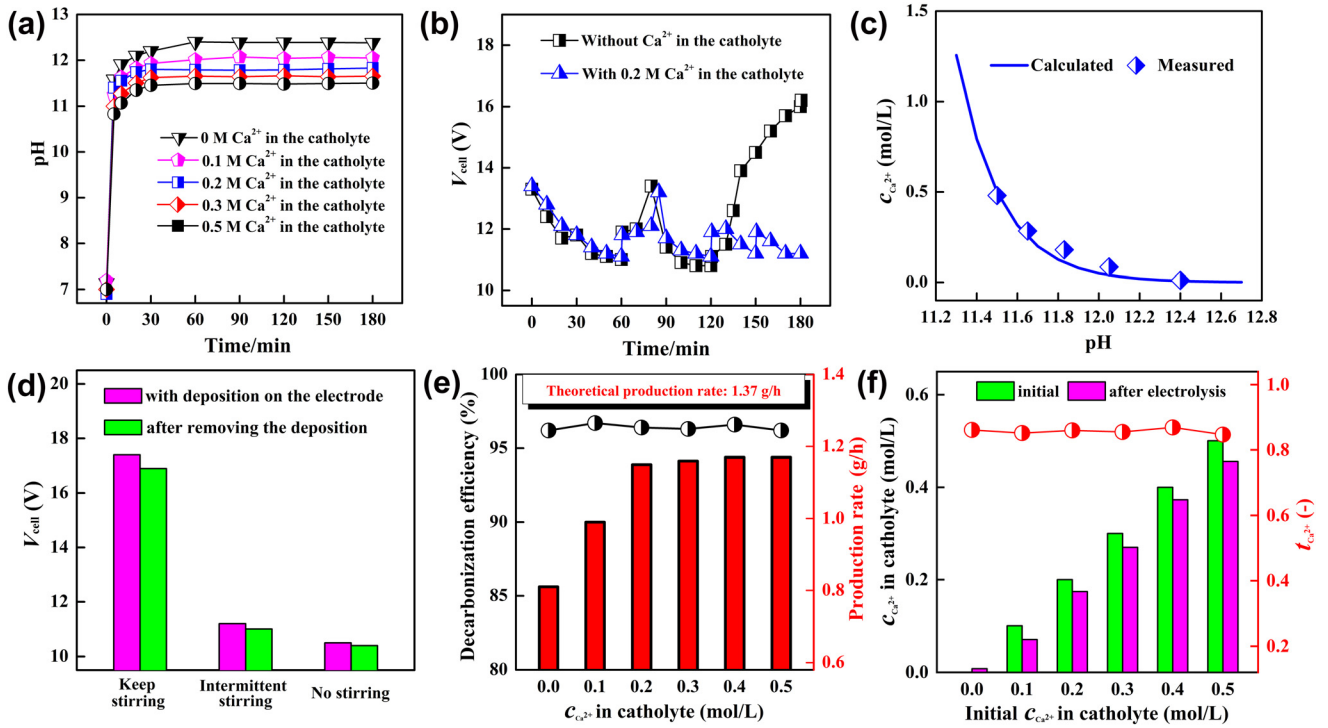

Fig. 3 Operating characteristics of the electrochemical production process of $Ca(OH)_2$ at various catholyte pH values using 0.5 M $Ca(NO_3)_2$ solution as the anolyte. (a) Evolution of the catholyte pH with time at various Ca^{2+} concentrations in 1 M $NaNO_3$ solution. (b) Voltage–time curves for the cement clinker precursor electrolyzer with and without Ca^{2+} in the catholyte. (c) Ca^{2+} concentration–pH correlation curve in $Ca(OH)_2$ saturated solutions. (d) Cell voltage change before and after removing the deposits from the electrode with 0.2 M Ca^{2+} in the catholyte. (e) Measured decarbonization efficiency and production rate based on $CaCO_3$ consumption and $Ca(OH)_2$ output (collected from the cathode chamber, membrane and electrode), respectively. (f) Changes of the Ca^{2+} concentration in the catholyte after electrolysis for 3 h and the calculated Ca^{2+} transference number ($t_{Ca^{2+}}$) at various catholyte compositions.

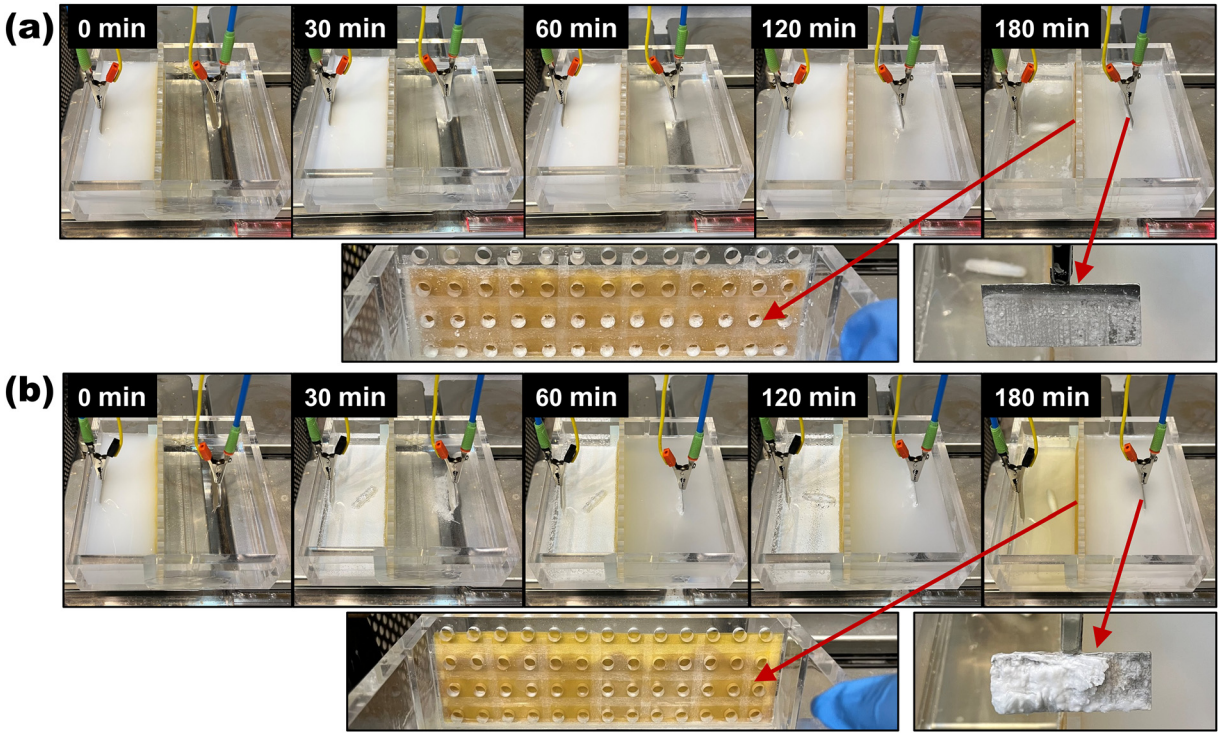

Fig. 4 Time-lapse images of the cement clinker precursor electrolyzer showing the precipitation process of $Ca(OH)_2$ during electrolysis and the precipitation behavior of the $Ca(OH)_2$ product on the membrane and electrode after 3 h of electrolysis at various Ca^{2+} concentrations in the catholyte. (a) Without Ca^{2+} and (b) with 0.2 M Ca^{2+} in the initial catholyte.

Based on this correlation as well as the solubility product constant of $Ca(OH)_2$ (5×10^{-6}), the Ca^{2+} concentration and pH value at equilibrium were calculated to be 0.008 mol L^{-1} and 12.4, respectively. The pH value is the same as the measured one in this work. In this case, the Ca^{2+} solubility in the catholyte is extremely low (0.32 g L^{-1}), which means that the entered Ca^{2+} cannot remain stable and will immediately precipitate once it passes through the membrane. The Ca^{2+} concentration–pH relationship curve in $Ca(OH)_2$ saturated solution indicates that it is possible to control the pH in the cathode chamber using Ca^{2+}-containing electrolytes (Fig. 3c). Therefore, we conducted another series of electrochemical experiments using catholytes with various initial Ca^{2+} concentrations to verify this hypothesis. The major difference observed after introducing Ca^{2+} into the catholyte is that the precipitation process was significantly enhanced, especially near the electrode, as shown in Fig. 4b and Movie S2.† Besides, this operation fundamentally avoids the precipitate accumulation on the membrane, making the membrane clean and clear throughout the electrolysis (Fig. 4b). Instead, the adhesion of products on the electrode becomes very significant. This is because the higher initial Ca^{2+} concentration leads to an evident reduction of the catholyte pH (Fig. 3a) and ensures high Ca^{2+} capacity in the catholyte (Fig. 3c). This change enables the successful transport of Ca^{2+} through the membrane, while the OH^- produced at the cathode will immediately react with the surrounding Ca^{2+}, leading to product enrichment near the electrode. Fortunately, it did not show a significant impact on the conductivity as only 1–3% fluctuation in voltage was measured before and after removing the deposits from the electrode (Fig. 3d). Moreover, the deposit thickness remained stable during electrolysis owing to the forced convection flow induced by H_2 bubble evolution.[15] More importantly, it is easier to clean electrodes than membranes because the latter usually show a microporous structure and a low mechanical strength.

The production rate of $Ca(OH)_2$ is a key index for the proposed electrochemical method because it determines the economic benefit of the process. Although the anode current efficiency was proved to be ~100% in many studies,[15–17] they all failed to directly measure the mass of the produced $Ca(OH)_2$ owing to its significant adhesion on the membrane and the porous electrode. Another reason for this research gap may be that they found the current efficiency for the electrochemical production of $Ca(OH)_2$ unsatisfactory. In this work, the large size of the separator channel and the flat structure of the electrode make it possible to collect all of the products and calculate the production rate (Fig. 3e). After washing, separation, and drying, we analyzed them using powder XRD and confirmed all the products to be $Ca(OH)_2$ (Fig. 5a). The SEM images show that the $Ca(OH)_2$ products are made up of hexagonal crystals. They show a much finer morphology when produced at higher initial concentrations of Ca^{2+}, with the average particle size decreasing from 10 μm to less than 3 μm (Fig. 5b). From the crystal growth standpoint,[26] high initial concentrations of metal ions lead to fast crystal growth compared to

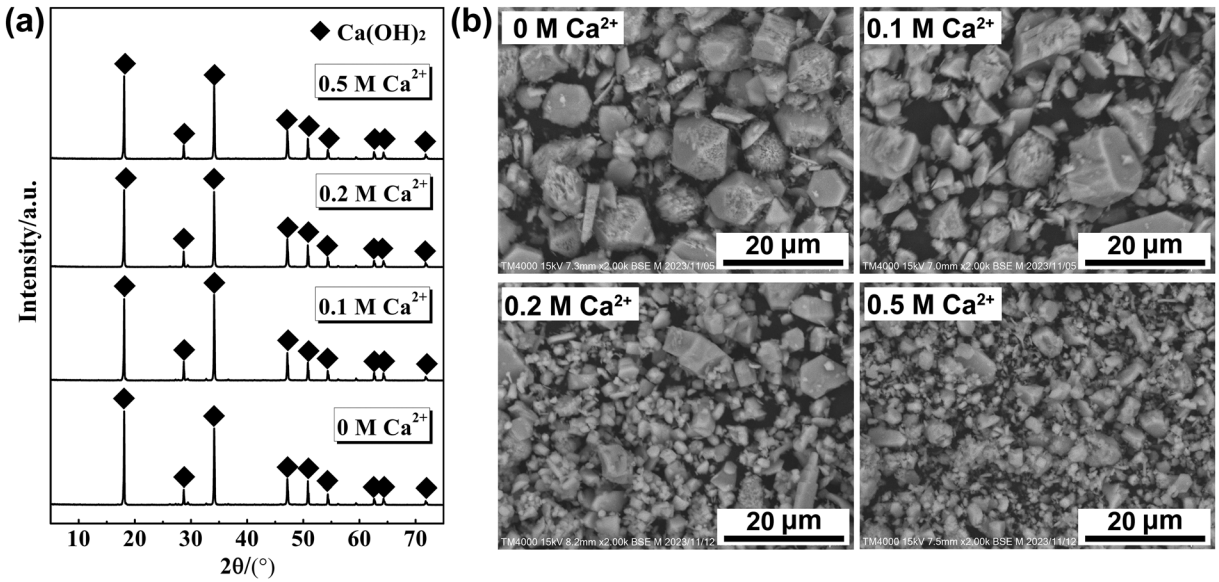

Fig. 5 (a) XRD patterns and (b) SEM images of the precipitation products collected from the cathode chamber, membrane and electrode after electrolysis at various Ca^{2+} concentrations in the initial catholyte.

low initial concentrations but give a relatively small crystal size. Note that the electrochemically produced $Ca(OH)_2$ has bigger sizes and a more homogeneous distribution than those obtained from the conventional precipitation method (Fig. S4a, S4b and S4c†), suggesting effective grain growth of the product during electrolysis. Although no other peaks were detected in the XRD pattern, the TG-DTA analysis reveals the presence of some $CaCO_3$ impurity (~7%) in the product since an obvious mass loss is observed at 500–700 °C (Fig. S4d†).[27] This impurity may not come from the reaction with CO_2 produced in the cell because it was also detected in $Ca(OH)_2$ powder obtained by the conventional alkaline precipitation method. The carbonation reaction is more likely to occur during the drying of the $Ca(OH)_2$ slurry.

The Ca^{2+} concentration in the catholyte shows no impact on the decarbonization efficiency of $CaCO_3$ (~96%), but it leads to a significant difference in the production rate of $Ca(OH)_2$ (Fig. 3e). $Ca(OH)_2$ was produced at a rate of 810 mg h^{-1} when using a Na-salt as the sole electrolyte, whose current efficiency is only 59% (the maximum value is 1370 mg h^{-1} under a constant current of 1 A assuming that all the charge is used for generating $Ca(OH)_2$). The production rate shows a remarkable increase with the initial Ca^{2+} concentration and remains stable at around 1150 mg h^{-1} when the concentration is over 0.2 M, corresponding to 84% of the theoretical efficiency. The lower pH in the presence of Ca^{2+} means less accumulation of OH^- in the cathode chamber, promoting $Ca(OH)_2$ precipitation. However, this difference is only responsible for a 5% change in the production rate according to a rough calculation (0 *vs.* 0.2 M Ca^{2+}). A mass loss is inevitable during the precipitate collection process from the channels of the separator, but it is far from enough to explain the difference in the product output.

According to Faraday's law, the quantity of OH^- produced during electrolysis is the same in all cases because it predominantly depends on the current. This demonstrates that the drop in $Ca(OH)_2$ production at higher pH is caused by the shortage of Ca^{2+}. When a conventional Na- or K-salt is used as the catholyte, all the Ca^{2+} ions for $Ca(OH)_2$ generation are from the anode chamber. In this case, the precipitation process will be affected by the Ca^{2+} transport across the membrane. In this work, the Ca^{2+} concentration in the catholyte shows an evident decline after electrolysis (Fig. 3f), and the Ca^{2+} transference number is only ~0.85 despite the presence of a CEM. From this point, introducing Ca^{2+} into the catholyte is necessary because it eliminates the risk of production stagnation. Note that there is a certain gap between the practical and theoretical production rate even when a Ca^{2+}-containing catholyte is used (84% *vs.* 100%). The constant pH suggests excellent reaction kinetics in both chambers, where the produced H^+ and OH^- can react instantly with $CaCO_3$ and Ca^{2+}, respectively. Therefore, the yield gap may be caused by the mass loss during collection, washing, and filtration, and the non-ideal Ca^{2+} transference number.

3.3 Problems and prospects

Although our findings demonstrate a considerable advancement over the previous studies, several issues should be addressed in future work. First, not all the Ca^{2+} ions dissolved from the feedstock are transported to the cathode chamber, leading to a non-ideal Ca^{2+} transference number. This means that the product partially came from the reaction with the added electrolyte, causing a decrease in the Ca^{2+} concentration in the catholyte and a negative impact on the continuous electrolysis operation. Therefore, future work should focus on the optimization of the Ca^{2+} transference number. Second, natural

limestone is used in cement production rather than pure $CaCO_3$ for economic viability. It is a challenge to prevent the dissolution and transport of impurity metal ions (such as Si^{4+}, Fe^{3+}, and Al^{3+}) if natural limestone is used in the electrochemical process.[28] According to many metal–water potential–pH diagrams, the leaching of impurity ions will become difficult under potentials. This behavior may enhance the selective extraction of Ca^{2+} during electrolysis and ensure the product purity and production rate. Third, dry-process cement manufacturing has a strict limit on the moisture content in the feedstock because it will affect the kiln's durability. This problem may occur if the feedstock changes from $CaCO_3$ to $Ca(OH)_2$ for cement production. In China, the use of carbide slag [$Ca(OH)_2$ slurry] as the main feedstock in dry-process cement plants is reasonably mature. In this process, a drying system is added to the precalciner to remove the free and crystal water. It reduces the stress of the kilns and is a good example of the application of electrochemical cement clinker precursors.

4. Conclusions

In summary, we developed a two-chamber membrane-based cement clinker precursor electrolyzer that operates at variable pH values, and the role of electrolyte pH in $CaCO_3$ decarbonization, Ca^{2+} transport, and $Ca(OH)_2$ precipitation was investigated. High pH caused by using a Na- or K-salt as the catholyte is the key reason for membrane clogging, leading to a continuous voltage increase and an inferior production rate of $Ca(OH)_2$. The catholyte pH can be quantitatively modulated by controlling the initial Ca^{2+} concentration. This design ensures a clean membrane throughout the electrolysis and makes the deposits move from the membrane to the electrode, but it causes only a 1–3% fluctuation in the system voltage. The production rate reaches 84% of the theoretical limit due to the smooth transport and separation of Ca^{2+}, the highest ever reported in the literature. Another new finding is that the deposition is also significant on the anode side of the membrane under fast decarbonization kinetics with the pH maintained at 5.1 (~99% current efficiency), leading to a significant voltage increase. The periodic pH change in the anode chamber by intermittent stirring ensures a relatively flat voltage profile, although it leads to a sacrifice of ~3% decarbonization efficiency. This work provides a simple but effective approach for the durable and efficient production of electrochemical cement clinker precursors. Further research is required in the future to optimize the Ca^{2+} transference number, cathode current efficiency, and cell voltage, especially when natural limestone is used as the feedstock.

Author contributions

Lei Xu: methodology, investigation, validation, writing – original draft, and writing – review & editing. Lei Liu: conceptualization, funding acquisition, methodology, and supervision. Zheng Fang: data curation and investigation. Min Chen: resources and supervision. Guangfeng Ou: formal analysis and writing – review & editing. Michio Suzuki: data curation and resources. Yuya Sakai: resources, supervision, and writing – review & editing.

Data availability

The data are available from the corresponding author on reasonable request.

Conflicts of interest

The authors declare no competing financial interests.

Acknowledgements

The authors gratefully acknowledge the financial support from the 32nd Iron and Steel Institute of Japan (ISIJ) Research Promotion Grant and the National Natural Science Foundation of China (grant number 51804075). The authors would like to thank Ms Rieko Takeyama from the Department of Applied Biological Chemistry, the University of Tokyo, for supporting the ICP-MS measurement supported by JSPS (19H05771 and 23H00339) throughout this research.

References

1 L. Liu, G. Ou, L. Xu, N. Ogiwara, S. Uchida, H. Yang and Y. Sakai, Simultaneous productions of high-purity calcium carbonate and amorphous nanosized silica-rich gel from waste concrete powder by alkaline treatment and carbonation, *J. Environ. Manage.*, 2024, **372**, 123319, DOI: **10.1016/j.jenvman.2024.123319**.

2 L. D. Ellis, A. F. Badel, M. L. Chiang, R. J. Y. Park and Y. M. Chiang, Toward electrochemical synthesis of cement—An electrolyzer-based process for decarbonating $CaCO_3$ while producing useful gas streams, *Proc. Natl. Acad. Sci. U. S. A.*, 2020, **117**(23), 12584–12591, DOI: **10.1073/pnas.1821673116**.

3 International Energy Agency. Technology Roadmap—Low-Carbon Transition in the Cement Industry, April 2018. **https://www.iea.org/reports/technology-roadmap-low-carbon-transition-in-the-cement-industry**.

4 G. Habert, S. A. Miller, V. M. John, J. L. Provis, A. Favier, A. Horvath and K. L. Scrivener, Environmental impacts and decarbonization strategies in the cement and concrete industries, *Nat. Rev. Earth Environ.*, 2020, **1**(11), 559–573, DOI: **10.1038/s43017-020-0093-3**.

5 P. S. Fennell, S. J. Davis and A. Mohammed, Decarbonizing cement production, *Joule*, 2021, **5**(6), 1305–1311, DOI: **10.1016/j.joule.2021.04.011**.

6 S. A. Miller and F. C. Moore, Climate and health damages from global concrete production, *Nat. Clim. Change*, 2020, **10**(5), 439–443, DOI: 10.1038/s41558-020-0733-0.
7 E. Benhelal, E. Shamsaei and M. I. Rashid, Challenges against CO_2 abatement strategies in cement industry: A review, *J. Environ. Sci.*, 2021, **104**, 84–101, DOI: 10.1016/j.jes.2020.11.020.
8 A. Hasanbeigi, L. Price and E. Lin, Emerging energy-efficiency and CO_2 emission-reduction technologies for cement and concrete production: A technical review, *Renewable Sustainable Energy Rev.*, 2012, **16**(8), 6220–6238, DOI: 10.1016/j.rser.2012.07.019.
9 R. Snellings, Assessing, understanding and unlocking supplementary cementitious materials, *RILEM Tech. Lett.*, 2016, **1**, 50–55, DOI: 10.21809/rilemtechlett.2016.12.
10 M. Schneider, The cement industry on the way to a low-carbon future, *Cem. Concr. Res.*, 2019, **124**, 105792, DOI: 10.1016/j.cemconres.2019.105792.
11 F. Williams and A. Yang, Potential of reducing CO_2 emissions in cement production through altering clinker compositions, *Ind. Eng. Chem. Res.*, 2024, **63**(40), 17158–17167, DOI: 10.1021/acs.iecr.4c01885.
12 M. Paidar, V. Fateev and K. Bouzek, Membrane electrolysis—History, current status and perspective, *Electrochim. Acta*, 2016, **209**, 737–756, DOI: 10.1016/j.electacta.2016.05.209.
13 R. K. Miao, N. Wang, S. F. Hung, W. Y. Huang, J. Zhang, Y. Zhao, P. Ou, S. Wang, J. P. Edwards, C. Tian, J. Han, Y. Xu, M. Fan, J. E. Huang, Y. C. Xiao, A. H. Ip, H. Liang, E. H. Sargent and D. Sinton, Electrified cement production via anion-mediated electrochemical calcium extraction, *ACS Energy Lett.*, 2023, **8**(11), 4694–4701, DOI: 10.1021/acsenergylett.3c01668.
14 Q. Xie, L. Wan, Z. Zhang and J. Luo, Electrochemical transformation of limestone into calcium hydroxide and valuable carbonaceous products for decarbonizing cement production, *iScience*, 2023, **26**(2), 106015, DOI: 10.1016/j.isci.2023.106015.
15 Z. Zhang, B. A. W. Mowbray, C. T. E. Parkyn, C. Waizenegger, A. S. R. Williams, E. W. Lees, S. Ren, Y. Kim, R. P. Jansonius and C. P. Berlinguette, Cement clinker precursor production in an electrolyser, *Energy Environ. Sci.*, 2022, **15**(12), 5129–5136, DOI: 10.1039/D2EE02349K.
16 B. A. W. Mowbray, Z. B. Zhang, C. T. E. Parkyn and C. P. Berlinguette, Electrochemical cement clinker precursor production at low voltages, *ACS Energy Lett.*, 2023, **8**(4), 1772–1778, DOI: 10.1021/acsenergylett.3c00242.
17 Z. B. Zhang, Low-temperature electrochemical cement clinker production, *ACS Energy Lett.*, 2023, **8**(9), 3927–3934, DOI: 10.1021/acsenergylett.3c01211.
18 D. Ramirez-Amaya, P. Dreyse, N. P. Martínez, P. F. Troncoso, I. Navarrete, M. Noel, R. I. Canales and M. Gonzalez, Comparison of the electrochemical decarbonation of different-grade limestones used in cement manufacturing, *Cem. Concr. Res.*, 2023, **174**, 107307, DOI: 10.1016/j.cemconres.2023.107307.
19 G. E. Badea, C. Hora, I. Maior, A. Cojocaru, C. Secui, S. M. Filip and F. C. Dan, Sustainable hydrogen production from seawater electrolysis: through fundamental electrochemical principles to the most recent development, *Energies*, 2022, **15**(22), 8560, DOI: 10.3390/en15228560.
20 F. Xiao, T. Wu and Y. Yang, Research progress in hydrogen production by hydrolysis of magnesium-based materials, *Int. J. Hydrogen Energy*, 2024, **49**, 696–718, DOI: 10.1016/j.ijhydene.2023.07.085.
21 C. Pateraki, S. J. Andersen, D. Ladakis, A. Koutinas and K. Rabaey, Direct electrochemical extraction increases microbial succinic acid production from spent sulphite liquor, *Green Chem.*, 2019, **21**, 2401–2411, DOI: 10.1039/C9GC00361D.
22 M. Haug, F. Bouville, C. Ruiz-Agudo, J. Avaro, D. Gebauer and A. R. Studart, Cold densification and sintering of nanovaterite by pressing with water, *J. Eur. Ceram. Soc.*, 2020, **40**(3), 893–900, DOI: 10.1016/j.jeurceramsoc.2019.10.034.
23 T. Tong, A. F. Wallace, S. Zhao and Z. Wang, Mineral scaling in membrane desalination: Mechanisms, mitigation strategies, and feasibility of scaling-resistant membranes, *J. Membr. Sci.*, 2019, **579**, 52–69, DOI: 10.1016/j.memsci.2019.02.049.
24 T. Rinder, M. Dietzel and A. Leis, Calcium carbonate scaling under alkaline conditions – Case studies and hydrochemical modeling, *Appl. Geochem.*, 2013, **35**, 132–141, DOI: 10.1016/j.apgeochem.2013.03.019.
25 Z. Zhang, A. S. R. Williams, S. Ren, B. A. W. Mowbray, C. T. E. Parkyn, Y. Kim, T. Ji and C. P. Berlinguette, Electrolytic cement clinker precursor production sustained through orthogonalization of ion vectors, *Energy Environ. Sci.*, 2025, **18**, 2395–2404, DOI: 10.1039/D4EE04881D, Advance Article.
26 G. H. Nancollas, The growth of crystals in solution, *Adv. Colloid Interface*, 1979, **10**(1), 215–252, DOI: 10.1016/0001-8686(79)87007-4.
27 L. Xu, Y. Liu, M. Chen, N. Wang, H. Chen and L. Liu, Production of green, low-cost and high-performance anorthite-based ceramics from reduced copper slag, *Constr. Build. Mater.*, 2023, **375**, 130982, DOI: 10.1016/j.conbuildmat.2023.130982.
28 Z. Fang, G. Xiong, Z. Shao, S. Zhou, G. Ou, L. Liu, M. Suzuki, C. Wang and Y. Sakai, Electrochemical recycling of recycled concrete powder: Selective recovery of calcium and silica to enable sustainable construction materials, *Resour. Environ. Sustain.*, 2024, **18**, 100182, DOI: 10.1016/j.resenv.2024.100182.